Stretching of buckled filaments by thermal fluctuations

Krzysztof Baczynski, Reinhard Lipowsky, and Jan Kierfeld

Max Planck Institute of Colloids and Interfaces, Science Park Golm, D-14424 Potsdam, Germany
(Received 6 August 2007; published 21 December 2007)

We study the buckling instability of filaments or elastic rods in two spatial dimensions in the presence of thermal fluctuations. We present an analytical solution based on a renormalizationlike procedure where we integrate out short wavelength fluctuations in order to obtain an effective theory governing the buckling instability. We calculate the resulting shift of the critical force by fluctuation effects and the average projected filament length parallel to the force direction as a function of the applied force and of the contour length of the filament. We find that, in the buckled state, thermal fluctuations lead to an *increase* in the mean projected length of the filament in the force direction. As a function of the contour length, the mean projected length exhibits a cusp at the buckling instability, which becomes rounded by thermal fluctuations. Our analytic results are confirmed by Monte Carlo simulations.

I. INTRODUCTION

Buckling of elastic rods is a ubiquitous mechanical problem, which is relevant in elasticity theory and mechanical engineering [1]. An elastic rod undergoes a buckling instability if the compressional force F exceeds a certain threshold value, the critical force F_c, for constant rod length or if the rod length L exceeds a certain critical length L_c for constant force. Such buckling instabilities also play a role in biological systems, whenever rigid filaments or semiflexible polymers, such as cytoskeletal filaments or DNA, are under a compressive load. In a living cell compressive loads can be generated by the polymerization of filaments or by molecular motors, both of which are driven by hydrolysis of adenine triphosphate (ATP) [2]. Both processes can generate forces in the piconewton range. On the other hand, biological nanorods also show pronounced thermal shape fluctuations, which give rise to a number of interesting cooperative phenomena [3]. Therefore thermal fluctuations should influence the buckling behavior of filaments as well.

It has been shown experimentally that polymerization forces are sufficient to buckle microtubules of micrometer length [4]. In Ref. [4], the shape of buckled microtubules growing against a hard obstacle has been analyzed to measure microtubule polymerization forces, which were found to lie in the piconewton range. Forces in the piconewton range can also be generated by motor proteins, and it has also been demonstrated experimentally that molecular motors can buckle microtubules of micrometer length [5]. Experiments on microtubules growing inside lipid vesicles demonstrate that microtubules also buckle under the compressive forces exerted by a lipid bilayer under tension [6]. All these experiments show that small forces in the piconewton range are sufficient to buckle cytoskeletal filaments. Such small buckling forces suggest that additional thermal forces, which also generate piconewton forces on a nanometer scale, could modify the buckling instability considerably.

Some extensions of the classical buckling instability have been considered before. The buckling of twisted filaments, which is relevant to many biological filaments, has been studied in Ref. [7]. For charged polymers the buckling instability is related to the collapse of a stiff polyelectrolyte under the action of attractive intrachain interactions, which has also been analyzed in the presence of thermal fluctuations [8]. Also the dynamics of buckling rods has been investigated theoretically [9,10].

The effect of thermal fluctuations on the buckling instability, on the other hand, has received much less attention. The strength of thermal fluctuations of semiflexible polymers is characterized by their persistence length $L_p = \kappa/T$ ($k_B \equiv 1$) [11]. On length scales larger than the persistence length a semiflexible polymer decays into uncorrelated Kuhn segments of length $2L_p$ and becomes an effectively flexible polymer with no resistance to buckling, i.e., the critical buckling force vanishes. In this paper, we will focus on the semiflexible regime $L \ll L_p$, where the buckling instability is still governed by a nonzero threshold force but strongly modified by thermal fluctuations. The only discussion of thermal fluctuations on the buckling instability has been given by Odijk [12] in the framework of a harmonic approximation for filaments in three spatial dimensions. In a similar semiclassical approximation the influence of quantum fluctuations on buckling instabilities has been studied [13].

In this paper, we will systematically consider the influence of anharmonic corrections for buckling in two spatial dimensions, which can be realized experimentally in confined geometries, i.e., for filaments adsorbed or confined to a planar substrate. We use a systematic expansion in the ratio L/L_p of contour length to persistence length, and integrate out small scale fluctuations to obtain an effective theory governing the buckling instability. We calculate the shift of the buckling force in the presence of thermal fluctuations and find that the buckling force *increases* in two dimensions in contrast to the perturbative result of Odijk for three spatial dimensions [12]. We also calculate the mean projected length as a function of the applied force (at fixed contour length) and as a function of the contour length (at fixed applied force) in the presence of thermal fluctuations. Our results show that thermal fluctuations lead to a *stretching* of buckled filaments, whereas they compress unbuckled filaments.
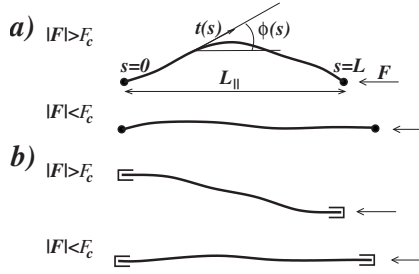
FIG. 1. Thermally fluctuating filament under a compressive force **F** for (a) free and (b) clamped boundary conditions at both ends. For absolute values $|\mathbf{F}|$ of the force larger than the critical buckling force F_c the filament is buckled; for forces smaller than F_c it remains unbuckled. The filament has contour length L, $\mathbf{t}(s)$ is the unit tangent vector, and $\phi(s)$ is the corresponding tangent angle at arc length s. $L_\parallel$ is the projected length in the force direction.

II. MODEL

An inextensible semiflexible polymer or filament of contour length L in d spatial dimensions is governed by the general wormlike chain Hamiltonian as given by

$$\mathcal{H} = \int_0^L ds \left[\frac{\kappa}{2}(\partial_s \mathbf{t})^2 - \mathbf{F} \cdot \mathbf{t}(s) \right], \tag{1}$$

where s is the arc length and $\mathbf{t}(s)$ are the unit tangent vectors of the contour with $|\mathbf{t}(s)|=1$, see Fig. 1. **F** is a homogeneous external force, which will be taken to be compressive in the following. The Hamiltonian (1) only contains contributions from the bending energy and the external force and applies to inextensible filaments without torsional degrees of freedom.

There is a close analogy between the Hamiltonian (1) for a filament in d spatial dimensions and a one-dimensional magnetic system of d-component magnetic spins. The Hamiltonian (1) with the constraint $|\mathbf{t}(s)|=1$ is equivalent to a nonlinear σ model in one dimension in an external field for a d-component spin vector of unit length; the compressive force plays the role of an external magnetic field, which acts to reverse the magnetization. In this analogy the buckling instability corresponds to the onset of magnetization reversal upon reversal of the magnetic field, and the critical threshold force F_c for buckling is analogous to the coercive magnetic field. In the context of magnetic systems, it is well known that there is no ordered phase in one-dimensional systems *in the thermodynamic limit* of infinite system size. Thus for the buckling instability it is crucial that we consider a *finite* system. This is reflected in the result $F_{c,0} \sim \kappa/L^2$ for the critical buckling force at zero temperature, which vanishes in the thermodynamic limit of large lengths L.

In two spatial dimensions we can fulfill the constraint $|\mathbf{t}(s)|=1$ explicitly by using a parametrization in terms of the tangent angle $\phi(s)$, i.e., $\mathbf{t}(s)=(\cos \phi(s), \sin \phi(s))$. The Hamiltonian becomes

$$\mathcal{H} = \int_0^L ds \left[\frac{\kappa}{2}(\partial_s \phi)^2 + F \cos \phi(s) \right], \tag{2}$$

where $F \equiv |\mathbf{F}|$ is the absolute value of the compressive force. We consider the buckling instability of the straight state

$\phi(s)=0$ and the compressive force is acting in the direction $\phi=\pi$. An important quantity, which can serve as an order parameter for the buckling instability, is the projected length $L_\parallel$, which is given by

$$L_\parallel = \int_0^L ds \cos \phi(s). \tag{3}$$

III. BUCKLING AT ZERO TEMPERATURE

The classical buckling instability is obtained by minimizing the total energy (2) with respect to the angle configuration $\phi(s)$. This minimization leads to the beam equation

$$\kappa \partial_s^2 \phi + F \sin \phi(s) = 0 \tag{4}$$

which has to be solved for appropriate boundary conditions. Boundary conditions at each end of the rod can be classified as free or clamped, where "free" means that the tangent at the end point can freely adapt to the compressional force and "clamped" means that it is constrained to a certain direction, which is usually parallel to the applied force. In the following, we will focus on boundary conditions with two clamped or two free ends. In two dimensions, as considered here, we use either clamped boundary conditions $\phi(0)=\phi(L)=0$ with both tangent vectors (anti)parallel to the applied force or free boundary conditions, which correspond to $\partial_s\phi(0)=\partial_s\phi(0)=0$, i.e., a vanishing curvature and thus a vanishing torque at the filament ends.

Solving the beam Eq. (4) one finds that a nonzero buckled solution exists at zero temperature above a critical buckling force $F_{c,0}$, which is given by

$$F_{c,0} = \pi^2 \kappa / L^2 \tag{5}$$

both for free and clamped ends and fixed contour length L. Alternatively, if the filament polymerizes against a fixed compressive load F, it will buckle above a critical contour length

$$L_{c,0} = \pi(\kappa/F)^{1/2} \tag{6}$$

at zero temperature.

Energy minimization gives the contour length L as well as the projected length $L_\parallel$ as a function of the maximal buckling angle ϕ^*, which is attained at $s=0$ or $s=L$ for two free ends and for $s=L/2$ for two clamped ends,

$$\frac{L}{L_{c,0}} = \sqrt{\frac{F}{F_{c,0}}} = \frac{\mathcal{I}_1(\phi^*)}{\mathcal{I}_1(0)}, \tag{7}$$

$$\frac{L_\parallel}{L_{c,0}} = \frac{\mathcal{I}_1(\phi^*) - \mathcal{I}_2(\phi^*)}{\mathcal{I}_1(0)} \tag{8}$$

with the two integrals

$$\mathcal{I}_1(y) \equiv \int_0^y dx \frac{1}{\sqrt{2(\cos x - \cos y)}} \tag{9}$$

and
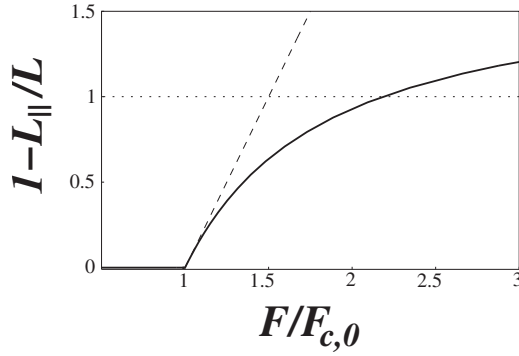
FIG. 2. Reduced projected length $L_\parallel/L$ as a function of the reduced force $F/F_{c,0}$. For $F < F_{c,0}$, the filament is straight with $L_\parallel = L$ and $1 - L_\parallel/L = 0$. The buckled solution appears for $F > F_{c,0}$. The solid curve is obtained numerically from relations (7) and (8) by a parametric plot using the buckling angle ϕ^* as the curve parameter. The dashed line is the linear approximation (12). For $F/F_{c,0} > 2.183$, $L_\parallel$ becomes negative.

$$\mathcal{I}_2(y) \equiv \int_0^y dx \, \frac{1 - \cos x}{\sqrt{2(\cos x - \cos y)}}. \qquad (10)$$

As y goes to zero, the first integral has the finite limit $\mathcal{I}_1(0) = \pi/2$ whereas $\mathcal{I}_2(0) = 0$. Relations (7) and (8) can also be used as implicit equations to determine the buckling angle ϕ^* for given contour length L or projected length $L_\parallel$, respectively.

Using Eqs. (7) and (8), one can obtain parametric representations of the reduced projected length $L_\parallel/L$ or $L_\parallel/L_{c,0}$ as a function of the reduced force or the reduced contour length,

$$\bar{F} \equiv F/F_{c,0} \quad \text{and} \quad \bar{L} \equiv L/L_{c,0}, \qquad (11)$$

in the buckled state with $F > F_{c,0}$ or $L > L_{c,0}$, see Figs. 2 and 3, where we use the buckling angle ϕ^* as a curve parameter.
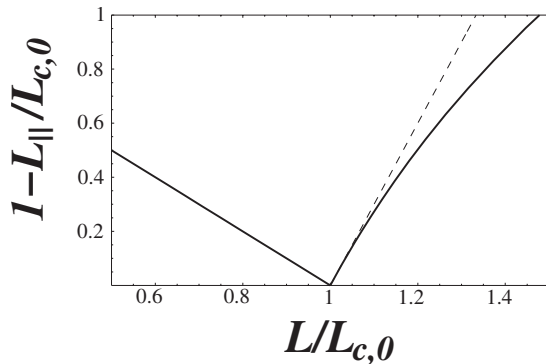
FIG. 3. Reduced projected length $L_\parallel/L_{c,0}$ as a function of the reduced contour length $L/L_{c,0}$. For $L < L_{c,0}$, the filament is straight with $L_\parallel = L$ which corresponds to the left part of the diagram with $L/L_{c,0} < 1$. The buckled solution appears for $L > L_{c,0}$. The solid curve is obtained numerically by a parametric plot using the buckling angle ϕ^* as the curve parameter in Eqs. (7) and (8). The dashed line is the linear approximation (12). For $L/L_{c,0} > 1.478$, $L_\parallel$ becomes negative.

Close to the buckling instability we find the asymptotic behavior

$$1 - L_\parallel/L \approx 2(\bar{F} - 1) \quad \text{for small } \bar{F} - 1 > 0,$$

$$1 - L_\parallel/L_{c,0} \approx 3(\bar{L} - 1) \quad \text{for small } \bar{L} - 1 > 0. \qquad (12)$$

For $L < L_{c,0}$, on the other hand, the filament is unbuckled which implies that the projected length $L_\parallel$ is identical with the contour length L and

$$1 - L_\parallel/L_{c,0} = 1 - \bar{L} \quad \text{for } \bar{L} - 1 < 0. \qquad (13)$$

Combining the two results for $L > L_{c,0}$ and $L < L_{c,0}$, we see that the relation between projected and contour length exhibits a cusp at the buckling point with $L = L_{c,0}$ [3], as shown in Fig. 3. The cusp could be used to detect the buckling threshold in experiments on growing filaments under a fixed compressive load, which could be generated, for example, by optical traps. The parametric representations shown in Figs. 3 and 2 and thus the asymptotic behavior (12) just above the buckling threshold are valid both for two free and two clamped ends.

IV. BUCKLING IN THE PRESENCE OF THERMAL FLUCTUATIONS

In order to consider the effects of thermal fluctuations on the buckling instability, several approaches are possible. We can expand around the "classical" configuration obtained in the previous section and integrate out fluctuations up to quadratic (or higher) order. This approach, however, does not allow us to calculate a fluctuation-induced shift of the threshold force for buckling. Therefore we employ a renormalizationlike procedure where we integrate out short wavelength fluctuations in order to obtain an effective theory governing the long wavelength buckling instability. We focus on the regime close to the buckling instability where we can expand the Hamiltonian (2) in tangent angles up to quartic order, and obtain

$$\mathcal{H} = \int_0^L ds \left[\frac{\kappa}{2} (\partial_s \phi)^2 + F \left(1 - \frac{1}{2} \phi^2(s) + \frac{1}{24} \phi^4(s) \right) \right]. \qquad (14)$$

For free and clamped boundary conditions, Fourier expansion of $\phi(s)$ leads to

$$\phi(s) = \sum_{n=1}^N \widetilde{\phi}_n \cos(n\pi s/L) \quad \text{(free)}, \qquad (15)$$

$$\phi(s) = \sum_{n=1}^N \widetilde{\phi}_n \sin(n\pi s/L) \quad \text{(clamped)}, \qquad (16)$$

respectively, with Fourier coefficients $\widetilde{\phi}_n$. The maximal wave number N is given by the number of degrees of freedom, $N = L/a$, where a is a microscopic cutoff, which is set by the monomer size or the filament diameter. The $n = 0$ mode is absent for free boundary conditions because we apply the

additional constraint $z(L)-z(0)=\int_0^L ds \sin \phi(s)=0$ that the end points have the same height coordinate (perpendicular to the force direction). This constraint is automatically fulfilled by the zero temperature solution but has to be imposed separately in the presence of thermal fluctuations. The condition $\tilde{\phi}_0=0$ satisfies this constraint up to terms of order $\mathcal{O}(\tilde{\phi}_n^3)$.

In order to investigate the effect of the anharmonic quartic terms, we write the Hamiltonian (14) as

$$\mathcal{H} = \mathcal{H}_2 + \mathcal{H}_4, \qquad (17)$$

where $\mathcal{H}_2$ contain all terms up to quadratic order and $\mathcal{H}_4$ the remaining terms up to quartic order. Using the Fourier expansions (15) or (16), the quadratic part can be rewritten as

$$\mathcal{H}_2\{\tilde{\phi}_n\} = FL + \sum_{n\geq 1} \frac{F_{c,0}L}{4}(n^2-\bar{F})\tilde{\phi}_n^2. \qquad (18)$$

This representation in Fourier modes shows that buckling is an instability of the $n=1$ mode for $\bar{F}>1$, which attains a nonzero equilibrium value in this regime at zero temperature. Higher modes $n>1$ remain stable up to higher order buckling forces, i.e., for $\bar{F}<n^2$. In the following we focus on the regime $\bar{F}\lesssim 4$ where only the $n=1$ mode can become unstable and large. Expectation values for higher modes $n,m\geq 2$,

$$\langle \tilde{\phi}_n \tilde{\phi}_m \rangle = \delta_{nm}\frac{2T}{F_{c,0}L}\frac{1}{n^2-\bar{F}}, \qquad (19)$$

as calculated with the Hamiltonian (18) are of the order of

$$\frac{T}{F_{c,0}L} = \frac{1}{\pi^2}\frac{L}{L_p} \equiv t. \qquad (20)$$

The dimensionless parameter t is a reduced temperature, which is small for semiflexible filaments with $L\lesssim L_p$. Expectation values $\langle \tilde{\phi}_n^2 \rangle \sim t$ of higher modes are thus small as well. The parameter t will be used in the following as an expansion parameter for the systematic treatment of fluctuations. This parameter is small in the limit of small temperature, large bending rigidity, or small contour length. A typical value for a microtubule of contour length $L=10$ μm and $L_p=1$ mm is $t\simeq 10^{-3}$, whereas an actin filament of contour length $L=10$ μm and $L_p=15$ μm has a much larger value, $t\simeq 6.7\times 10^{-2}$.

This motivates our treatment of the quartic Hamiltonian $\mathcal{H}_4$. Because fluctuations of higher Fourier modes $n\geq 2$ will remain small at the buckling transition we neglect terms of cubic and quartic order in the Fourier modes $n\geq 2$. The corresponding terms for the unstable $n=1$ mode have to be retained, and we obtain

$$\mathcal{H}_4\{\tilde{\phi}_n\}/T = \frac{\bar{F}}{64t}\tilde{\phi}_1^4 \pm \frac{\bar{F}}{48t}\tilde{\phi}_1^3\tilde{\phi}_3 + \sum_{n\geq 2}\frac{\bar{F}}{16t}(\tilde{\phi}_1^2\tilde{\phi}_n^2 \pm \tilde{\phi}_1^2\tilde{\phi}_n\tilde{\phi}_{n+2}). \qquad (21)$$

The upper and lower signs in Eq. (21) are for free and clamped boundary conditions, respectively.

We first trace over all higher order modes $n\geq 2$ in order to obtain an effective Hamiltonian for the single mode $n=1$,

which is the relevant mode for the buckling instability:

$$e^{-\mathcal{H}_{\mathrm{eff}}\{\tilde{\phi}_1\}/T} = \left(\prod_{n\geq 2}\int_{-\infty}^{\infty}d\tilde{\phi}_n\right)e^{-\mathcal{H}_2\{\tilde{\phi}_n\}/T-\mathcal{H}_4\{\tilde{\phi}_n\}/T}. \qquad (22)$$

The Hamiltonian $\mathcal{H}_2+\mathcal{H}_4$ as given by Eqs. (18) and (21) is quadratic in the higher order modes and the Gaussian integrals in Eq. (22) can be performed to obtain

$$\mathcal{H}_{\mathrm{eff}}\{\tilde{\phi}_1\}/T = \bar{F}/t + \alpha\tilde{\phi}_1^2 + \beta\tilde{\phi}_1^4 \qquad (23)$$

with

$$\alpha \equiv \frac{1}{4}\left(\frac{1-\bar{F}}{t} + \frac{1}{2}h(\bar{F})\right), \qquad (24)$$

$$h(\bar{F}) \equiv \sum_{n\geq 2}\frac{\bar{F}}{n^2-\bar{F}}, \qquad (25)$$

$$\beta \equiv \frac{1}{64}\frac{\bar{F}}{t} \qquad (26)$$

to leading order in the small parameter t. We point out that to this order there is no difference between clamped and free boundary conditions. Therefore our results regarding the critical force and the mean projected length will be identical for both types of boundary conditions also in the presence of thermal fluctuations. The function $h(\bar{F})$ can be approximated by $h(\bar{F}) \simeq \sqrt{\bar{F}} \operatorname{arccoth}(2/\sqrt{\bar{F}})$ by converting the sum into an integral. Close to the buckling threshold around $\bar{F}=1$ we can also find an exact expression for the Taylor expansion $h(\bar{F}) \approx 3/4+(1-\bar{F})(\pi^2/12+1/16)$. For $t\ll 1$ we can therefore use

$$\alpha \approx \frac{1}{4}\left(\frac{3}{8} + \frac{1-\bar{F}}{t}\right) \qquad (27)$$

to a good approximation.

A. Critical force

The resulting effective theory (23) for the single mode $\tilde{\phi}_1$ is a fourth order Ginzburg-Landau-type theory. The buckling instability occurs if the coefficient $\alpha(\bar{F})$ of the quadratic term changes sign. This determines the critical force F_c in the presence of thermal fluctuations,

$$F_c = F_{c,0}\left(1 + \frac{t}{2}h(\bar{F}_c)\right) \approx F_{c,0}\left(1 + \frac{3t}{8}\right), \qquad (28)$$

where the last approximation is to leading order in the reduced temperature t such that $h(\bar{F}_c)\approx h(1)=3/4$. Using the relation $\bar{F}=\bar{L}^2$, we obtain the corresponding result for the critical contour length L_c in the presence of thermal fluctuations,

$$\bar{L}_c = \sqrt{\bar{F}_c} \approx 1 + \frac{3t}{16} \qquad (29)$$

to leading order in t.

It is remarkable that, in two dimensions as considered so far, the critical buckling force *increases* because of fluctuation effects as described by Eq. (28). In the special case of two dimensions, the short wavelength fluctuations always *weaken* the effect of the applied force on a larger scale because the fourth order contribution to the force term in the Hamiltonian (14) has a sign opposite to the leading quadratic contribution. We can define an effective compressive force $F_{\text{eff}}(L)$ for the mode $n=1$ of wavelength L by rewriting the coefficient α of the quadratic term of the effective theory (23) in an analogous form as the $n=1$ term in the original Hamiltonian (18),

$$\alpha = \frac{1}{4t}(1 - \bar{F}_{\text{eff}}). \tag{30}$$

This effective compressive force is *smaller* than the original force,

$$\bar{F}_{\text{eff}}(L) = \bar{F} - \frac{t}{2}h(\bar{F}) < \bar{F}, \tag{31}$$

as can be read off from Eq. (24). On the other hand, it is well known that short wavelength fluctuations do *not* affect the bending rigidity on a larger scale in two dimensions because there is no bending rigidity renormalization in two dimensions for the continuous wormlike chain model (2) [11]. Thus the effective buckling threshold $F_{\text{eff},c}(L)$ is not affected by short wavelength fluctuations, and $F_{\text{eff},c}(L) = F_{c,0} = \pi^2 \kappa / L^2$. The condition that the effective force needs to be sufficient to buckle the filament becomes $F_{\text{eff}}(L) > F_{\text{eff},c}(L) = F_{c,0}$. Since the effective force is smaller than the "bare" force according to relation (31), this condition is equivalent to an increase of the bare critical buckling force: $F_c > F_{c,0}$. Because the bending rigidity is renormalized toward smaller values in dimensions $d > 2$ [11], this argument only applies to two spatial dimensions.

The argument can be generalized to arbitrary spatial dimensions by considering the behavior of the bending rigidity κ and the force F under the action of the renormalization group (RG) transformation, which has been worked out in the context of the equivalent nonlinear σ model [14]. The continuous RG flow equations for the equivalent one-dimensional and d-component nonlinear σ model under an infinitesimal change of the length scale by a factor $b = 1 + d\ell$ are

$$\frac{d\kappa}{d\ell} = -\kappa + \frac{2-d}{2\pi\Lambda}T, \tag{32}$$

$$\frac{dF}{d\ell} = F - \frac{d-1}{4\pi\Lambda}\frac{FT}{\kappa}, \tag{33}$$

where $\Lambda \sim 1/a$ is a large scale momentum cutoff. The buckling instability is governed by the dimensionless force $\bar{F} = F/F_{c,0} = FL^2/\pi^2\kappa$. Using the RG flow Eqs. (32) and (33) (and the trivial flow under rescaling, $dL/d\ell = -L$), we find the RG equation for the dimensionless force,

$$\frac{d\bar{F}}{d\ell} = \frac{L^2}{\pi^2\kappa}\frac{dF}{d\ell} - \frac{FL^2}{\pi^2\kappa^2}\frac{d\kappa}{d\ell} + 2\frac{FL}{\pi^2\kappa}\frac{dL}{d\ell} \tag{34}$$

$$= \frac{d-3}{4\pi}\frac{1}{L_p\Lambda}\bar{F}, \tag{35}$$

i.e., $d\bar{F}/d\ell < 0$ for $d < 3$ and $d\bar{F}/d\ell > 0$ for $d > 3$. The effective dimensionless force for a mode of wavelength L is obtained by following the RG flow from the bare initial dimensionless force, $\bar{F}(0) = \bar{F}$, to the logarithmic scale $\ell = \ln(L/a)$, where $\bar{F}_{\text{eff}}(L) = \bar{F}(\ln(L/a))$. The condition for buckling in the presence of thermal fluctuations is $\bar{F}_{\text{eff}}(L) > 1$. If $d\bar{F}/d\ell < 0$ small fluctuations weaken the effective force as compared to the buckling threshold and an increased bare force is needed to achieve buckling, as in our above argument for two dimensions. The RG treatment thus shows that critical force F_c in the presence of thermal fluctuations should be increased by thermal fluctuations for all dimensions $d < 3$, i.e., $F_c > F_{c,0}$, whereas it decreases for dimensions $d > 3$, i.e., $F_c < F_{c,0}$. The three-dimensional case $d = 3$ is marginal, and higher order terms in the RG equations would need to be considered. For three spatial dimensions it has been argued by Odijk that the critical force decreases in the presence of thermal fluctuations [12] based on a calculation up to quadratic order.

The RG Eq. (34) shows that the behavior of the critical buckling force in the presence of thermal fluctuations is a result of two competing effects: (i) The decrease of the effective compressive force by thermal fluctuations, which is present in all dimensions $d > 1$ according to the RG Eq. (33), and (ii) the softening of the filament by thermal fluctuations, which decreases the renormalized bending rigidity in dimensions $d > 2$, as can be seen from the RG Eq. (32). The softening of the filament for $d > 2$ is related to the existence of out-of-plane fluctuations, which lead to additional anharmonic terms governing the fluctuations of azimuthal angles. The weakening of the effective force (i) gives rise to an increase in the critical buckling force and dominates for dimensions $d < 3$, whereas the softening of the filament (ii) leads to a decrease of the critical buckling force and dominates in dimensions $d > 3$.

B. Mean projected length

The partition sum Z is obtained by performing the one-dimensional integral over the remaining Fourier amplitude mode $\tilde{\phi}_1$,

$$Z = \int_{-\infty}^{\infty} d\tilde{\phi}_1 e^{-\mathcal{H}_{\text{eff}}\{\tilde{\phi}_1\}/T}. \tag{36}$$

The partition sum defines the free energy $G \equiv -T \ln Z$. If the force dependence $G = G(F)$ is known the mean value of the projected filament length $L_\parallel$ from Eq. (3) can be determined from the relation

$$\langle L_\parallel \rangle = \partial_F G(F) = -T\partial_F \ln Z(F). \tag{37}$$

The remaining integral over $\tilde{\phi}_1$ in Eq. (36) gives
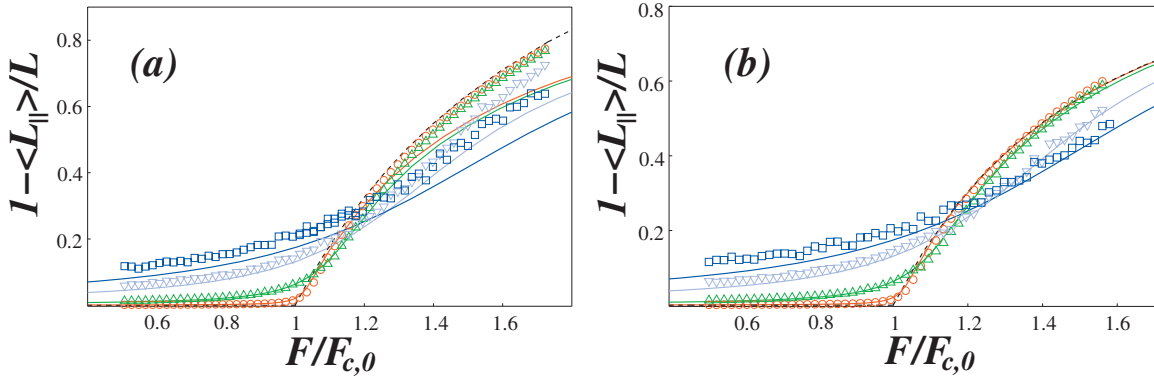
FIG. 4. (Color) Reduced projected length $\langle L_\parallel \rangle / L$ as a function of the reduced force $F/F_{c,0}$ for $L_p/L=100$ (red, $\bigcirc$), 10 (green, $\triangle$), 2 (light blue, $\triangledown$), and 1 (blue, $\square$) corresponding to $t \simeq 10^{-3}$, 10^{-2}, 5×10^{-2}, and 10^{-1}. The solid curves show the analytic result (41). (a) Comparison with Monte Carlo simulation data for two clamped ends using the full model (2). The dashed line corresponds to the zero temperature solution from Fig. 2. (b) Comparison with Monte Carlo simulation data for two clamped ends using the fourth order approximation of Eq. (14). The analytical zero temperature solution $1-L_\parallel/L=1-\bar{F}^{-2}$ is included as a dashed line.

$$Z = e^{\bar{F}/t} \int_{-\infty}^{\infty} d\tilde{\phi}_1 e^{-\alpha \tilde{\phi}_1^2 - \beta \tilde{\phi}_1^4} = \beta^{-1/4} \mathcal{F}(\alpha \beta^{-1/2}) \qquad (38)$$

with

$$\mathcal{F}(y) \equiv \frac{1}{2} \sqrt{|y|} e^{y^2/8} K_{1/4}(y^2/8) \quad \text{for } y > 0,$$

$$\mathcal{F}(y) \equiv \frac{1}{2} \sqrt{|y|} e^{y^2/8} \frac{\pi}{\sqrt{2}} [I_{1/4}(y^2/8) + I_{-1/4}(y^2/8)] \quad \text{for } y < 0,$$
$$(39)$$

where $I_\nu(x)$ and $K_\nu(x)$ denote the modified Bessel functions [15]. The parameters α and β are given by Eqs. (24) and (26), respectively. The mean projected length is obtained by differentiating expression (38) with respect to the force according to Eq. (37). For the reduced mean projected length $\langle L_\parallel \rangle / L$ we finally obtain

$$1 - \frac{\langle L_\parallel \rangle}{L} = t \left[-\frac{\partial_{\bar{F}} \beta}{4\beta} + \frac{\mathcal{F}'(\alpha/\beta^{1/2})}{\mathcal{F}(\alpha/\beta^{1/2})} \left(\frac{\partial_{\bar{F}} \alpha}{\beta^{1/2}} - \frac{\alpha \partial_{\bar{F}} \beta}{2\beta^{3/2}} \right) \right].$$
$$(40)$$

We further evaluate this expression using the approximation (27) for α, which leads to the following dependence on the reduced force $\bar{F}$:

$$1 - \frac{\langle L_\parallel \rangle}{L} = -\frac{t}{4\bar{F}} - \mathcal{F}_1 \left(\frac{\alpha}{\beta^{1/2}} \right) \frac{t^{1/2}}{\bar{F}^{3/2}} (\bar{F}_c + \bar{F}) \qquad (41)$$

with

$$\frac{\alpha}{\beta^{1/2}} \approx \frac{2}{t^{1/2} \bar{F}^{1/2}} (\bar{F}_c - \bar{F}), \qquad (42)$$

where

$$\mathcal{F}_1(y) \equiv \frac{\mathcal{F}'(y)}{\mathcal{F}(y)} = \frac{y}{4} \left(1 - \frac{K_{3/4}(y^2/8)}{K_{1/4}(y^2/8)} \right) \quad \text{for } y > 0,$$

$$\mathcal{F}_1(y) \equiv \frac{y}{4} \left(1 + \frac{I_{3/4}(y^2/8) + I_{-3/4}(y^2/8)}{I_{1/4}(y^2/8) + I_{-1/4}(y^2/8)} \right) \quad \text{for } y < 0$$
$$(43)$$

is a monotonously increasing, negative function. The solid curves in Fig. 4 show the result (41) for $1-\langle L_\parallel \rangle / L$ as a function of the reduced force $\bar{F}$ for different values of the parameter t.

For $\bar{F} < \bar{F}_c$ and $t \ll (\bar{F}_c - \bar{F})^2$, we use the asymptotic behavior to find the asymptotic behavior $\mathcal{F}_1(y) \approx -1/2y$ for $y \gg 1$ and obtain

$$1 - \frac{\langle L_\parallel \rangle}{L} \approx \frac{t}{2(\bar{F}_c - \bar{F})}, \qquad (44)$$

which is reminiscent of the shortening of a free filament by thermal fluctuations $1-\langle L_\parallel \rangle / L \approx \langle \phi^2 \rangle / 2 \sim t$. For $\bar{F} > \bar{F}_c$ and $t \ll (\bar{F}_c - \bar{F})^2$ we use $\mathcal{F}_1(-y) \approx -y/2 + 5y/16$ for $y \gg 1$ and obtain the asymptotics

$$1 - \frac{\langle L_\parallel \rangle}{L} \approx 1 - \left(\frac{\bar{F}_c}{\bar{F}} \right)^2 - \frac{t}{4\bar{F}} \left(1 + \frac{5}{8} \frac{\bar{F}_c + \bar{F}}{\bar{F} - \bar{F}_c} \right), \qquad (45)$$

which describes the suppression of thermal fluctuations and the approach to the zero temperature solution $1-L_\parallel/L=1-\bar{F}^{-2}$ in the strongly buckled state. Note that this zero temperature solution differs from the results of Sec. III, which are shown in Fig. 2, because of the expansion of the full Hamiltonian (2) up to fourth order in Eq. (14). The asymptotics (44) and (45) show that thermal fluctuations as described by the small parameter t *decrease* the mean projected length $\langle L_\parallel \rangle$ below its zero temperature value $L_\parallel = L$ for $\bar{F} < \bar{F}_c$ whereas they *increase* the mean projected length above the zero temperature value $L_\parallel = L\bar{F}^{-2}$ in the buckled state for $\bar{F} > \bar{F}_c$.
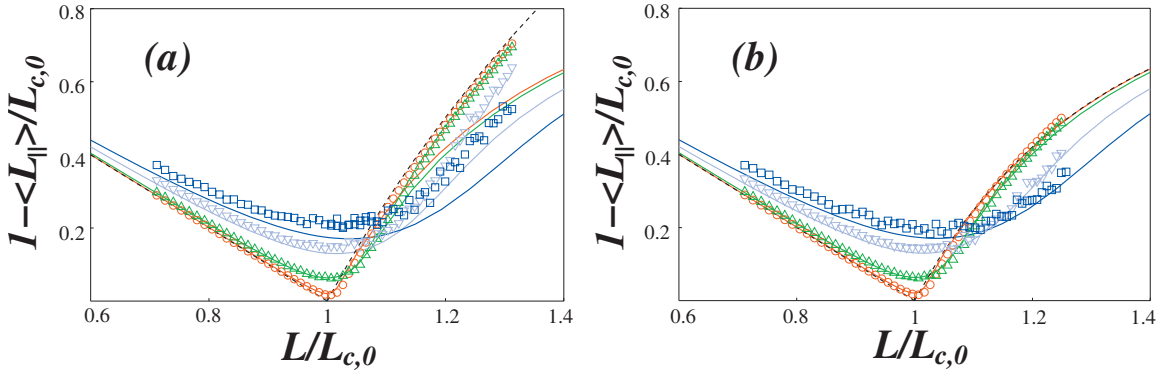
FIG. 5. (Color) Reduced projected length $\langle L_\parallel \rangle / L_{c,0}$ as a function of the reduced contour length $L/L_{c,0}$ for $L_p/L = 100$ (red, ○), 10 (green, △), 2 (light blue, ▽), and 1 (blue, □) corresponding to $t \simeq 10^{-3}$, 10^{-2}, 5×10^{-2}, and 10^{-1}. The solid curves show the analytic result. (a) Comparison with Monte Carlo simulation data for two clamped ends using the full model (2). The analytical zero temperature solution from Fig. 3 is shown as a dashed line. (b) Comparison with Monte Carlo simulation data for two clamped ends using the fourth order approximation of Eq. (14). The analytical zero temperature solution $1 - L_\parallel / L = 1 - \bar{L}^{-4}$ is included as a dashed line.

We thus conclude that thermal fluctuations lead to a stretching of buckled filaments, whereas they compress unbuckled ones. This implies that two curves for the mean projected length $\langle L_\parallel \rangle$ as a function of force, which are taken at different temperatures t, should *intersect* in the vicinity of the buckling force. This characteristic behavior is clearly confirmed in Fig. 4, where the full analytical result (41) is shown at different temperatures. The force value F_i of the intersection point of a projected length curve taken in the presence of thermal fluctuations with the zero temperature curve can be obtained approximately by expanding both curves around $\bar{F} = 1$. Using the expansion $\mathcal{F}_1(y) \approx a_0 + a_1 y$ for $y \ll 1$ with $a_0 = -\Gamma(3/4)/\Gamma(1/4) \simeq -0.34$ and $a_1 = 1/4 - a_0^2 \simeq 0.14$, where $\Gamma(x)$ is the gamma function [15], in Eq. (41) we find

$$1 - \frac{\langle L_\parallel \rangle}{L} \approx 2a_0 t^{1/2} + 4a_1(\bar{F} - 1) \qquad (46)$$

in the presence of thermal fluctuations and $1 - L_\parallel / L \approx 2(\bar{F} - 1)$ at zero temperature. Equating both results we obtain the intersection force

$$\bar{F}_i \approx 1 + \frac{2a_0}{1 + 4a_0^2} t^{1/2}. \qquad (47)$$

The intersection force F_i exceeds $F_{c,0}$ by a force $\sim t^{1/2} F_{c,0}$ and thus also exceeds F_c for small t, see Eq. (28). The increase of the force value for the intersection of the solid curves with the dashed black zero temperature curve with increasing t can also be clearly recognized in Fig. 4.

A characteristic feature of the buckling instability at zero temperature is the cusp in the relation between projected and contour length at the critical contour length $L_{c,0}$, see Fig. 3. For $L < L_{c,0}$ in the unbuckled state, the projected length is given by $L_\parallel = L$ and grows with the contour length. The projected length becomes maximal at the critical length $L = L_{c,0}$, where the filament buckles. If the filament grows further after buckling, $L > L_{c,0}$, the projected length decreases and $L_\parallel < L_{c,0}$. In the presence of thermal fluctuations, the cusp be-

comes modified, and we obtain the reduced mean projected length $1 - \langle L_\parallel \rangle / L_{c,0}$ as a function of the reduced contour length $\bar{L}$ by applying the relations $\bar{F} = \bar{L}^2$ and

$$1 - \frac{\langle L_\parallel \rangle}{L_{c,0}} = \left(1 - \frac{\langle L_\parallel \rangle}{L}\right) \bar{L} + (1 - \bar{L}) \qquad (48)$$

to our previous result (41). This gives

$$1 - \frac{\langle L_\parallel \rangle}{L_{c,0}} = 1 - \bar{L} - \frac{t}{4\bar{L}} - \mathcal{F}_1\left(\frac{\alpha}{\beta^{1/2}}\right) \frac{t^{1/2}}{\bar{L}^2} [\bar{L}_c^2 + \bar{L}^2] \qquad (49)$$

with

$$\frac{\alpha}{\beta^{1/2}} \approx \frac{2}{t^{1/2}\bar{L}} [\bar{L}_c^2 - \bar{L}^2]. \qquad (50)$$

The solid curves in Fig. 5 represent the expression $1 - \langle L_\parallel \rangle / L_{c,0}$ as a function of $\bar{L}$ according to Eq. (49). Thermal fluctuations lead to a rounding of the zero temperature cusp to a pronounced minimum and to a shift of the location $\bar{L}_m$ of this minimum. Because thermal fluctuations lead to a stretching of buckled filaments, whereas they compress unbuckled filaments, curves for different temperatures t intersect in Fig. 5. In principle, the contour length $\bar{L}_m$, where the mean projected length $\langle L_\parallel \rangle$ is maximal, could be determined experimentally by observing filaments growing against an obstacle as in Ref. [4]. A prediction for the value of $\bar{L}_m$ can be calculated from the result (49) by considering the limit $\alpha \beta^{-1/2} \ll 1$ and extending the Taylor expansion $\mathcal{F}_1(y) \approx a_0 + a_1 y + a_2 y^2 / 2$ for $y \ll 1$ to quadratic order with $a_2 = -|a_0|^3 \simeq -0.08$, which finally gives

$$\bar{L}_m \approx \bar{L}_c \left(1 + t^{1/2} \frac{8a_1 - 1 + 2a_0 t^{1/2}}{32a_2 + 24a_1 t^{1/2}}\right), \qquad (51)$$

i.e., the contour length $\bar{L}_m$, where the mean projected length $\langle L_\parallel \rangle$ becomes maximal, is shifted by a length $\sim t^{1/2}$ from the actual critical length L_c as given by Eq. (29) and the zero temperature critical length $L_{c,0}$. For small values $t \ll 1$, L_m is

a nonmonotonic function of t and first decreases to values $L_m < L_{c,0} < L_c$ before it becomes an increasing function of t and grows beyond L_c.

V. MONTE CARLO SIMULATIONS

In order to check our analytical predictions, we perform Monte Carlo simulations of buckling filaments in two dimensions in the presence of thermal fluctuations.

We simulate discretized versions of both the full Hamiltonian (2) and its fourth order approximation (14). In the simulations, we employ clamped boundary conditions. For free boundary conditions, the simulation is complicated by the fact that the filament "flips around" and reaches its trivial absolute minimum at $\phi(s) = \pi$ [for the Hamiltonian (2)] by thermal activation out of the metastable buckled state. In the configuration $\phi(s) = \pi$ the end points have crossed corresponding to a filament that is stretched rather than compressed by the force F.

In the Monte Carlo simulation we discretize the inextensible filament into N segments of fixed length $b \equiv L/N$ with angles $\phi_i \equiv \phi(ib)$. In order to equilibrate the filament, we use two kinds of Monte Carlo (MC) moves: (i) a local move in real space, which changes the angles of two neighboring segments $\phi_i \rightarrow \phi_i + \Delta\phi$ and $\phi_{i-1} \rightarrow \phi_{i-1} - \Delta\phi$ in opposite directions and thus induces a displacement of the point connecting both segments in the direction perpendicular to the local filament orientation; (ii) a collective move in Fourier space, which changes the amplitude $\tilde{\phi}_n$ of Fourier mode n by a random amount, $\tilde{\phi}_n \rightarrow \tilde{\phi}_n + \Delta\tilde{\phi}$. For the simulation results shown in Figs. 4 and 5, we used a discretization into $N = 200$ segments and performed 8×10^6 MC sweeps alternating local moves and moves in Fourier space.

The simulation results for the reduced projected length $\langle L_\parallel \rangle / L$ as a function of the reduced force $\bar{F}$ in Fig. 4 are in good agreement with our analytical result (41). Deviations become appreciable for the largest values of the reduced temperature $t \simeq 10^{-1}$ for which we performed simulations. For these values it becomes necessary to include higher order terms in the expansion in t underlying the analytical result (41). In particular, also the MC simulations confirm that curves for the mean projected length $\langle L_\parallel \rangle$ as a function of force, taken at different temperatures t, *intersect* in the vicinity of the buckling force. Also the MC results for the reduced projected length $\langle L_\parallel \rangle / L_{c,0}$ as a function of the reduced contour length $\bar{L}$ are in good agreement with the analytical result (49). The existence of a cusp rounded by thermal fluctuations close to the critical length L_c is clearly confirmed.

VI. CONCLUSION

We presented a systematic study of the buckling instability in the presence of thermal fluctuations in two spatial dimensions. By integrating over all short wavelength modes we derived an effective theory governing the buckling instability of the Fourier mode with the longest wavelength given by the filament length. We find that thermal fluctuations *increase* the critical force for buckling in two spatial dimensions. The increase in the critical buckling force is closely related to our main result that curves for the mean projected length $\langle L_\parallel \rangle$ measuring the end-to-end extension of the filament as a function of the applied compressive force, which are taken at different temperatures, *intersect* in the vicinity of the buckling force. This leads to the conclusion that thermal fluctuations lead to a stretching of buckled filaments, whereas they compress unbuckled filaments.

We presented arguments based on renormalization results for the nonlinear σ model which suggest that an increase in the critical force is found for all spatial dimensions $d < 3$, whereas the critical force should decrease for dimensions $d > 3$. The exact behavior in the marginal three-dimensional case remains an open question for future studies. It also remains an open question whether the effect of stretching by thermal fluctuations persists for spatial dimensions $d \geq 3$.

Our main result is the observation that a buckled filament stretches, i.e., increases its mean projected length in the direction of the applied force, upon increasing the temperature. This effect might have interesting consequences for a cross-linked network of filaments, which is under uniaxial compression such that a large fraction of filaments is buckled. The stretching of filaments by thermal fluctuations on the single filament level should lead to a *swelling* of the cross-linked filament network by thermal fluctuations. This is qualitatively different from the typical behavior of a network of flexible polymers, i.e., a rubberlike material, which stiffens and shrinks upon increasing the temperature [16]. The main reason for this qualitative difference lies in the role of entropy. Before buckling a filament is governed by entropy and an increasing temperature leads to a shortening of the filament in order to maximize its configurational entropy, similar to the well-known elastic behavior of a flexible polymer, which gives rise to classical rubber elasticity [16]. A buckled filament, on the other hand, is governed by its bending energy and for increasing temperature also the bending energy decreases in favor of the entropy, which gives rise to the observed effect of stretching by thermal fluctuations.

[1] L. Landau and E. M. Lifshitz, *Theory of Elasticity* (Pergamon, New York, 1986).

[2] J. Howard, *Mechanics of Motor Proteins and the Cytoskeleton* (Sinauer Associates, Inc., Sunderland, 2001).

[3] J. Kierfeld, P. Gutjahr, T. Kühne, P. Kraikivski, and R. Lipowsky, J. Comput. Theor. Nanosci. **3**, 898 (2006).

[4] M. Dogterom and B. Yurke, Science **278**, 856 (1997).

[5] F. Gittes, E. Meyhöfer, S. Baek, and J. Howard, Biophys. J. **70**, 418 (1996).

[6] M. Elbaum, D. Kuchnir Fygenson, and A. Libchaber, Phys. Rev. Lett. **76**, 4078 (1996).

[7] R. E. Goldstein and A. Goriely, Phys. Rev. E **74**, 010901(R) (2006).

[8] P. L. Hansen, D. Svensek, V. A. Parsegian, and R. Podgornik, Phys. Rev. E **60**, 1956 (1999).

[9] L. Golubovic, D. Moldovan, and A. Peredera, Phys. Rev. Lett. **81**, 3387 (1998).

[10] P. Ranjith and P. B. Sunil Kumar, Phys. Rev. Lett. **89**, 018302 (2002).

[11] P. Gutjahr, R. Lipowsky, and J. Kierfeld, Europhys. Lett. **76**, 994 (2006).

[12] T. Odijk, J. Chem. Phys. **108**, 6923 (1998).

[13] S. M. Carr, W. E. Lawrence, and M. N. Wybourne, Phys. Rev. B **64**, 220101(R) (2001).

[14] A. M. Polyakov, *Gauge Fields and Strings* (Harwood Academic Publishers, Chur, Switzerland, 1987); P. M. Chaikin and T. C. Lubensky, *Principles of Condensed Matter Physics* (Cambridge University Press, Cambridge, England, 1995).

[15] M. Abramowitz and A. I. Stegun, *Handbook of Mathematical Functions* (National Bureau of Standards, Washington, DC, 1965).

[16] L. R. G. Treloar, *The Physics of Rubber Elasticity* (Clarendon Press, Oxford, 1975).